Journal of Engineering Science 09(1), 2018, 1-10

JES
an international Journal

EFFECT OF RADIATION AND CONVECTIVE ENERGY FOR THE TRACK AND INTENSITY OF TROPICAL CYCLONES IN THE BAY OF BENGAL

A. Al-Mamun[1], M. M. Alam[2*] and H. R. Khan[1]
[1]Physics Discipline, Khulna University, Khulna, Bangladesh
[2]Department of Physics, Khulna University of Engineering & Technology (KUET), Bangladesh

Received: 11November 2017 Accepted: 18 December 2017

ABSTRACT

In the present research, Advanced Research WRF (ARW) model v3.2.1 has been used to study the effect of radiation and convective energy on the prediction of track and intensity of Tropical Cyclones (TC) in the Bay of Bengal (BoB) using six different microphysics schemes. Analysis has been made on the convective energies associated with tropical cyclones Sidr and Phailin, which formed over the Bay of Bengal and crossed Bangladesh and eastern coast of India in November 2007 and October 2013 respectively. The initial and boundary conditions of tropical cyclone are drawn from the global operational analysis and forecast products of National Center for Environmental Prediction (NCEP-GFS) available for the public at 1°×1° resolution. The model was run by using Kessler (KS), Lin et al. (Lin), WSM3-class simple ice, Ferrier (FE), WSM6-class graupel and Thomson (TH) graupel microphysics (MP) schemes coupling with different cumulus parameterization (CP) schemes and different initial conditions. The CP schemes used to simulate the TC's are Kain-Fritsch (KF) and Betts-Miller-Janjic (BMJ). The model domain consists of 8-24°N and 77-96°E and has 12 km horizontal resolution with 28 vertical sigma levels.

To examine the effect of outgoing long wave radiation (OLR), convective available potential energy (CAPE) and convective inhibition (CIN) for the intensity and track of tropical cyclone, four regions are considered inside the model domain. The regions are D1 (22-26°N and 87-93°E), D2 (18-22°N and 81-87°E), D3 (14-18°N and 78-84°E) and D4 (12-22°N and 84-94°E). The OLR has fallen in all four regions for both TCs, one day before landfall and has minimum in case of Sidr and Phailin in region D1 and D2 respectively compared to other regions. The area averaged CAPE has decreasing tendency in regions D2 and D3 for TC Phailin and D3, D4 for TC Sidr before landfall. The area averaged CIN has shown minimum in regions D2, D3 and D4 but maximum at D1 for Phailin before crossing the land. In case of Sidr CIN has found insignificant in four regions compare with Phailin.

Keywords: *CAPE, CIN, Cumulus Parameterization, Microphysics, OLR, WRF.*

1 INTRODUCTION

Tropical cyclone (TC) is a system of rapidly rotating storm with low pressure center, strong winds and spiral arrangement that produces heavy rain and storm surge. For this reason, coastal regions are particularly vulnerable to damage from a TC as compared to inland regions. Heavy rain, significant flooding inland, and storm surges can produce extensive coastal flooding up to 40 km inland from the coastline. Sobel and Camargo (2005) have found that outgoing long wave radiation (OLR) is low for the high vorticity and it has induced TCs activity by increasing sea surface temperature (SST). Pattanaik and Rama Rao (2009) simulated the characteristic of movement on a very severe cyclone Nargis using WRF-ARW model in the Bay of Bengal and have found that the tropical cyclones move towards the minimum OLR. Evans and water (2012) build up a relation between SST and OLR by using atmospheric-oceanic general circulation models (AOGCMs). They found that the OLR generally increases with increase in SST until a threshold ocean temperature is attained. Choi and Byun (2010) have shown that higher TC frequency indicate negative OLR. Choi and Moon (2012) have also observed that the TCs occurred in the western region of negative OLR. The OLR field shows a significant negative anomaly in the region over the North Indian Ocean (2013). Camargo *et al.,* (2007) have found that OLR minima at first TC positions and maxima at the position of maximum intensity.

Xu and Wang (2010) conducted many experiments and have shown that the removal of surface entropy fluxes outside the eyewall reduces the CAPE and suppresses the activity of spiral rainbands. Bogner *et al.* (1999) showed that CAPE value maximum at larger radii and lower near the eyewall. Smith and Montgomery (2012) have found that CAPE values are generally largest on the first day of observation and it decreased day by day. They also established an idea that CAPE varies inversely with CIN. Colon-Pagan (2009) found that near the center of TC, CAPE value is very low in their ARW model simulation. They worked on the Hurricane Jeanne in combination with four microphysics schemes and found that CAPE is associated with conditionally unstable airstreams, and around the prominent feeder bands CAPE is very low. Molinari and Vollaro (2009) using the more than 2000 dropsonde sounding by the NOAA Gulfstream-IV aircraft for observing the changing pattern of CAPE and found that the mean CAPE raises from center to outer region. The numerical experiment perform by the Fang *et al.* (2009) using the non hydrostatic, axisymmetric TC model and suggest that cyclone has increasing trend at first and decreasing trend when it is strengthen. Nolan *et al.* (2007) made a study on TC using WRF v2.1.2 combination of WSM6 class

* Corresponding Author: mdalam60@gmail.com

microphysics and Yonsei University (YSU) scheme which detected temperature effect on CAPE correspond with Coriolis force and showed that CAPE was proportional relation with SST.

In this research, many experiments have been conducted by using six different (Kessler, Lin *et al*., WSM3, Ferrier, WSM6 and Thompson) MP schemes in combination with KF and BMJ schemes considering different initial conditions for TCs Phailin (2013) and Sidr (2007). The effects of CAPE, CIN and OLR have been investigated for the movements and intensification of TCs in the Bay of Bengal.

2 DATA AND METHODOLOGY

Final Reanalysis (FNL) data (1^{o}x1^{o}) collected from National Center for Environment Prediction (NCEP) is used as initial and lateral boundary conditions (LBCs) which is updated at six hours interval i.e. the model is initialized with 0000, 0600, 1200 and 1800 UTC initial field of corresponding date. The NCEP FNL data is interpolated to the model horizontal and vertical grids and the model is integrated for 96 and 72-h period for TCs Sidr and Phailin. 24 experiments have been conducted in each case by using different microphysics schemes (e.g., Kessler, Lin *et al*., WSM3-class simple ice scheme, Ferrier, WSM6-class graupel scheme and Thompson graupel) in combinations with Kain-Fritsch (KF) and Betts-Miller-Janjic (BMJ) CP schemes with different initial conditions. In this regard, the initial conditions of 0000 UTC of 8 and 9 October 2013 have been considered for TC Phailin and initial conditions at 0000 UTC of 11 and 12 November 2007 for TC Sidr.

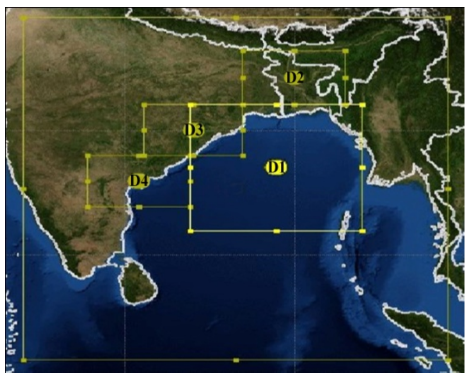

Figure 1: WRF Model simulated selected domain for TCs Phailin and Sidr

To examine the effect of radiation and energy on the intensity and track of tropical cyclone four regions are considered inside the model domain. The regions are D1 (22-26^{o}N and 87-93^{o}E), D2 (18-22^{o}N and 81-87^{o}E), D3 (14-18^{o}N and 78-84^{o}E) and D4 (12-22^{o}N and 84-94^{o}E). Four regions are separated to observe the effect of CAPE, CIN and OLR on the movement and track of tropical cyclones.

3 RESULTS AND DISCUSSION

The tracks of tropical cyclone Sidr and Phailin with different initial conditions and different microphysics and cumulus parameterization schemes are discussed in the following subsection. The CAPE, CIN and OLR of four different regions for the movement of these cyclones are also discussed in the following subsection.

3.1 Track of Tropical Cyclones Sidr and Phailin

The IMD and JTWC observed and WRF-ARW model simulated tracks for the period of 120-h and 96-h of TC Sidr for different MP schemes coupling with KF and BMJ schemes with the initial conditions at 0000 UTC on 11 and 12 November are displayed in Figure 2(a-d). The track forecasts are found reasonably accurate for different experiments i.e., up to the landfall time (landfall time of 1800 UTC of 15 November 2007). The significant deviations in tracks are observed among different MPs in combination with CP schemes. WSM3 and Kessler schemes in combination with KF and BMJ schemes have provided most deviated track with the initial conditions of 0000 UTC of 11 November and deviated towards left from the actual tracks of IMD and JTWC. At the time of landfall, Lin *et al.* and WSM6 schemes in combination with KF and BMJ schemes, Ferrier and Thompson schemes in combination with BMJ schemes have simulated less deviated track with the initial conditions of 0000 UTC of 11 November. The simulated tracks for all six MP schemes coupling with KF schemes have deviated significantly towards west from the original track with the initial conditions of 0000 UTC of 12 November. At the time of landfall, the track deviation is found minimum for Lin-BMJ and TH-BMJ combinations with the 0000 UTC of 12 November initial conditions. There is no landfall of TC Sidr up to the simulation time for WSM3 scheme in combination with KF and BMJ schemes with the initial conditions of 0000 UTC of 11 and 12 November 2007. The landfall time has almost matched for all MP schemes in combination with BMJ scheme, and Lin *et al*. and WSM6 schemes in combination with KF scheme for the initial conditions of 0000 UTC 11 November. The other combinations have shown positions delayed by 5-15h with the initial conditions of 0000 UTC 11 November.

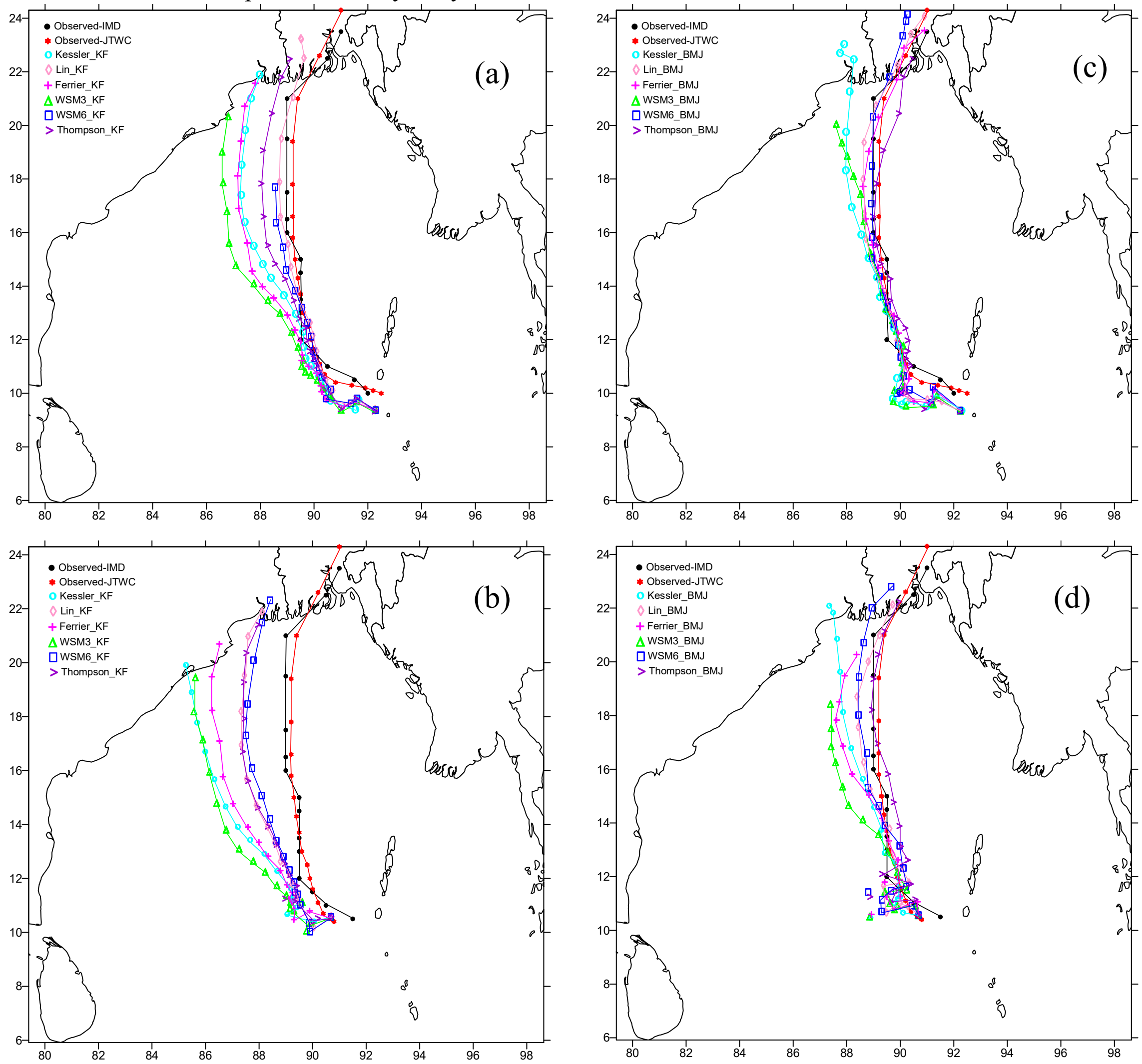

Figure 2: Simulated, IMD and JTWC observed track of tropical cyclone 'Sidr' using six different MP schemes coupling with (a-b) KF scheme and (c-d) BMJ scheme with the initial conditions of 0000 UTC of 11 and 12 November 2007.

The 120 and 96-h simulated and IMD observed tracks of TC Phailin for different cloud MP schemes in combination with KF and BMJ schemes with 0000 UTC of 8 and 9 October initial conditions are shown in Figure 3(a-d). It may be noted that roughly up to the landfall time (i.e., Official landfall is on 1700 UTC of 12 October 2013), the track forecasts for different sensitivity experiments have shown reasonably accurate prediction. WSM3-KF combinations have simulated most deviated track and Kessler-KF combinations have simulated less deviated track with the initial conditions at 0000 UTC of 8 October 2013. The simulated tracks for all MP schemes coupling with KF and BMJ schemes are found parallel to the observed tracks up to 0000 UTC of 12 October.

After that the simulated track followed the same path with the initial conditions at 0000 UTC of 8 October but the path of the cyclone shifted towards north. Due to this shifting the deviation increased after 0000 UTC of 12 October. The simulated tracks for Kessler-KF combination are shifted towards north from the observed tracks and all other MP schemes in combination with KF scheme, the landfall position is very near to the observed landfall position with the initial conditions of 0000 UTC of 9 October. Out of all MP schemes, the TH-KF combination simulated less deviated track at crossing point.

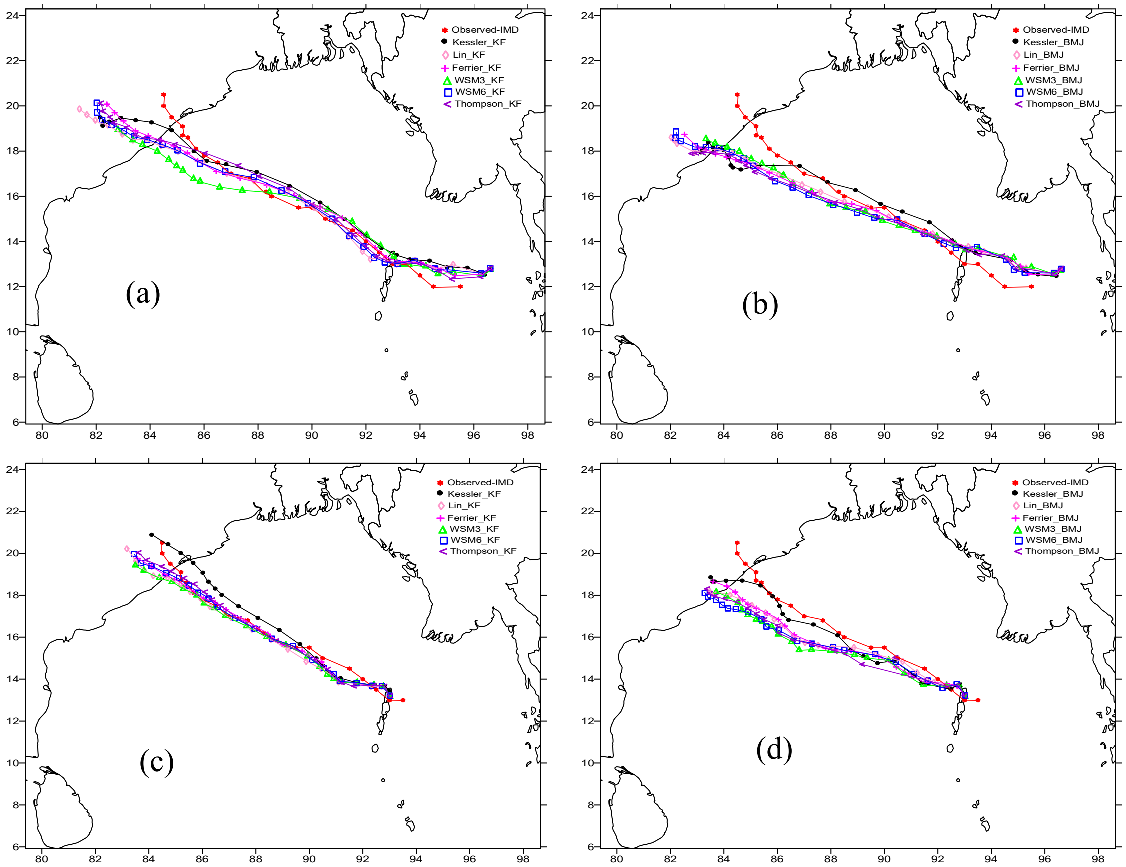

Figure 3: Model simulated and IMD Observed tracks of TC 'Phailin' using six different MP schemes coupling with (a-b) KF and (c-d) BMJ schemes with the initial conditions at 0000 UTC of 8 and 9 October 2013.

3.2 Intensity of TC Phailin

The 96-h storm intensity forecast in terms of minimum CSLP and maximum wind speed (m/s) at 10 m level using different MP schemes have presented in Figure 4(a-d). The simulated CSLP for all MP schemes in combination with KF scheme is much higher than that of BMJ scheme with the initial conditions at 0000 UTC of 9 October. IMD observed intensity is much lower than that of JTWC intensity in terms of pressure fall and 10 m level sustained wind. The IMD observed pressure fall are 22 hPa less than that of JTWC pressure fall and 10 m level wind is also less than that of JTWC wind speed by 12.7 m/s. The simulated pressure fall (10m sustained wind) with the 0000 UTC of 9 October initial conditions (Figure 4a) for all combination of MP schemes in combination with KF scheme is much higher (lower) than that of IMD observed results. BMJ scheme has simulated comparable pressure (Figure 4b) drop for all MP schemes up to 0600 UTC of 10 October but after that the model simulated pressure drop was much lower than that of observed pressure drop for 9 October initial condition. The model simulated faster fall of SLP up to 0300 and 1800 UTC of 10 October for BMJ and KF schemes respectively in combination with all MP schemes with the 9 October initial conditions. The simulated 10 m wind speed with the initial conditions at 0000 UTC of 9 October for all MP schemes coupling with KF (Figure 4c) and BMJ (Figure 4d) schemes were less than that of IMD and JTWC wind speed.

3-hourly minimum sea level pressure (MSLP) and associated maximum wind speed (m s^{-1}) at 10 m level using different MP schemes coupling with CP schemes are presented in Figures 5(a-d). IMD observed intensity (944 hPa, 58.8 m s^{-1}) of TC Sidr is much lower than that of JTWC intensity (918 hPa, 71.5 m s^{-1}) in terms of pressure fall and 10 m level sustained wind. The simulated pressure fall (Figure 5a) with the 0000 UTC of 12 November initial conditions Lin *et al.* scheme in combination with KF scheme are close to IMD observed results but lower than JTWC observed results. The simulated MSLP for all other MP schemes in combination with KF scheme lies between IMD and JTWC observed results with the initial conditions 0000 UTC of 12 November. The simulated pressure drop (Figure 5b) and wind speed (Figure 5d) for all MP schemes in combination with BMJ scheme are much lower than that of IMD and JTWC observed pressure and maximum wind speed with the initial condition of 0000 UTC of 12 November.

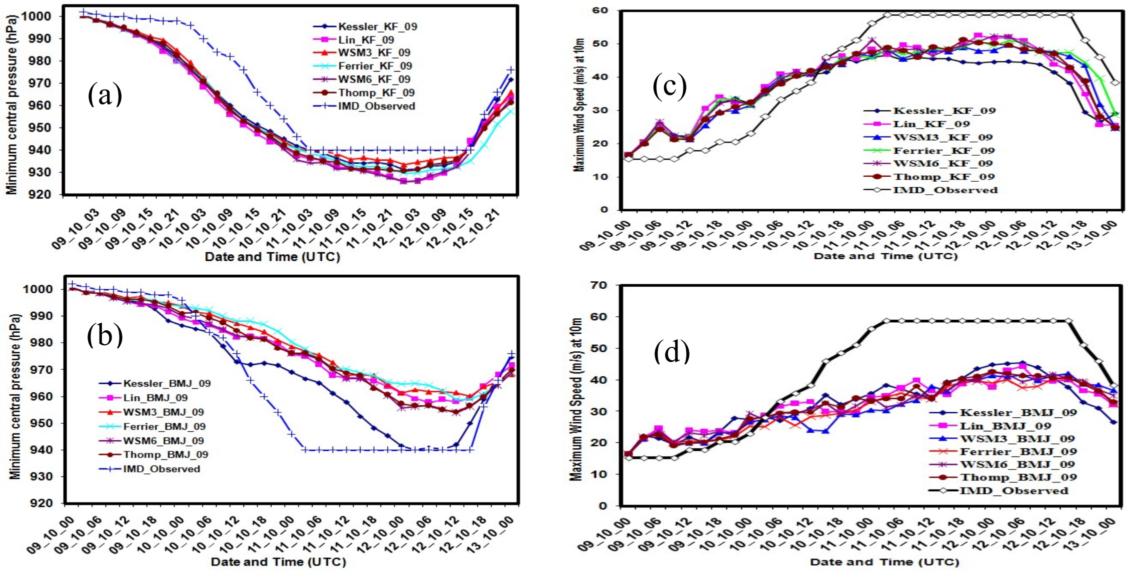

Figure 4: Model simulated and IMD observed (a-b) minimum CSLP and (c-d) maximum sustained wind at 10 m level of TC Phailin using six different MPs in combination with different CP schemes with the 0000 UTC of 9 October 2013 initial conditions.

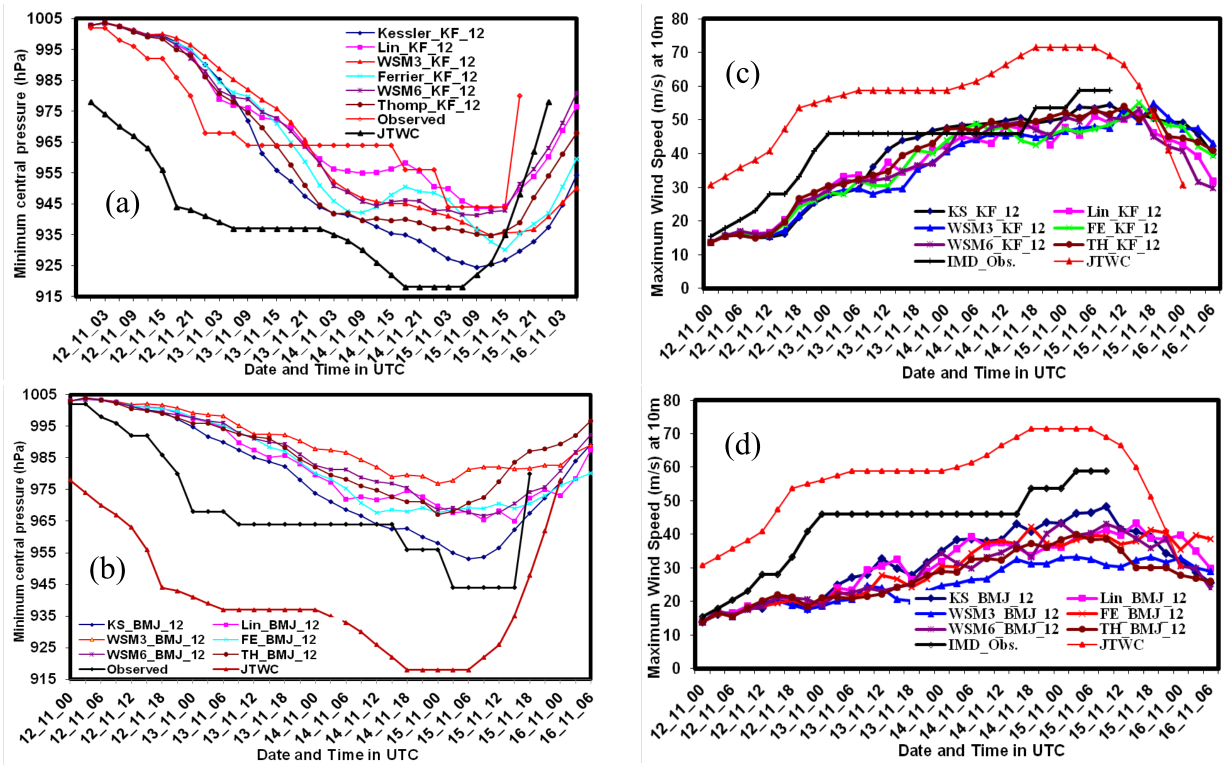

Figure 5: Model simulated (a-b) CSLP (hPa) and (c-d) maximum sustained wind at 10 m level of TC Sidr using six different MP schemes coupling with KF and BMJ schemes with initial conditions at 0000 UTC of 11 and 12 November 2007.

The wind speed simulated at 10 m level (Figure 5c) for all MP schemes coupling with KF scheme with the initial condition of 0000 UTC of 12 November are lower than that of JTWC observed wind speed and matched with IMD observed wind speed all through the simulation except maximum wind, which is less than that of IMD observed wind. BMJ scheme coupling with all MP schemes have simulated wind speed at 10 m level are much lower than that of IMD and JTWC observed wind with the initial condition at 0000 UTC of 12 November.

3.3 Outgoing Long Wave Radiation

The time varying area averaged OLR at four different regions such as D1, D2, D3 and D4 for all MPs in combination with KF scheme of TCs Phailin and Sidr are presented in Figure 6(a-h). In all regions, Kessler scheme in combination with KF scheme has simulated minimum and almost constant value of OLR. The area averaged OLR is found to have increasing pattern from 0000 UTC of 8 October to 0600 UTC of 9 October in region D1 of TC Phailin (Figure 6a). After that all MPs in combination with KF scheme have simulated a nearly linear pattern from 0600 UTC of 9 October to 0600 UTC of 11 October. The space averaged of OLR has varied in a sinusoidal pattern from 0600 UTC of 11 October up to the end of model run except FE and WSM3 schemes.

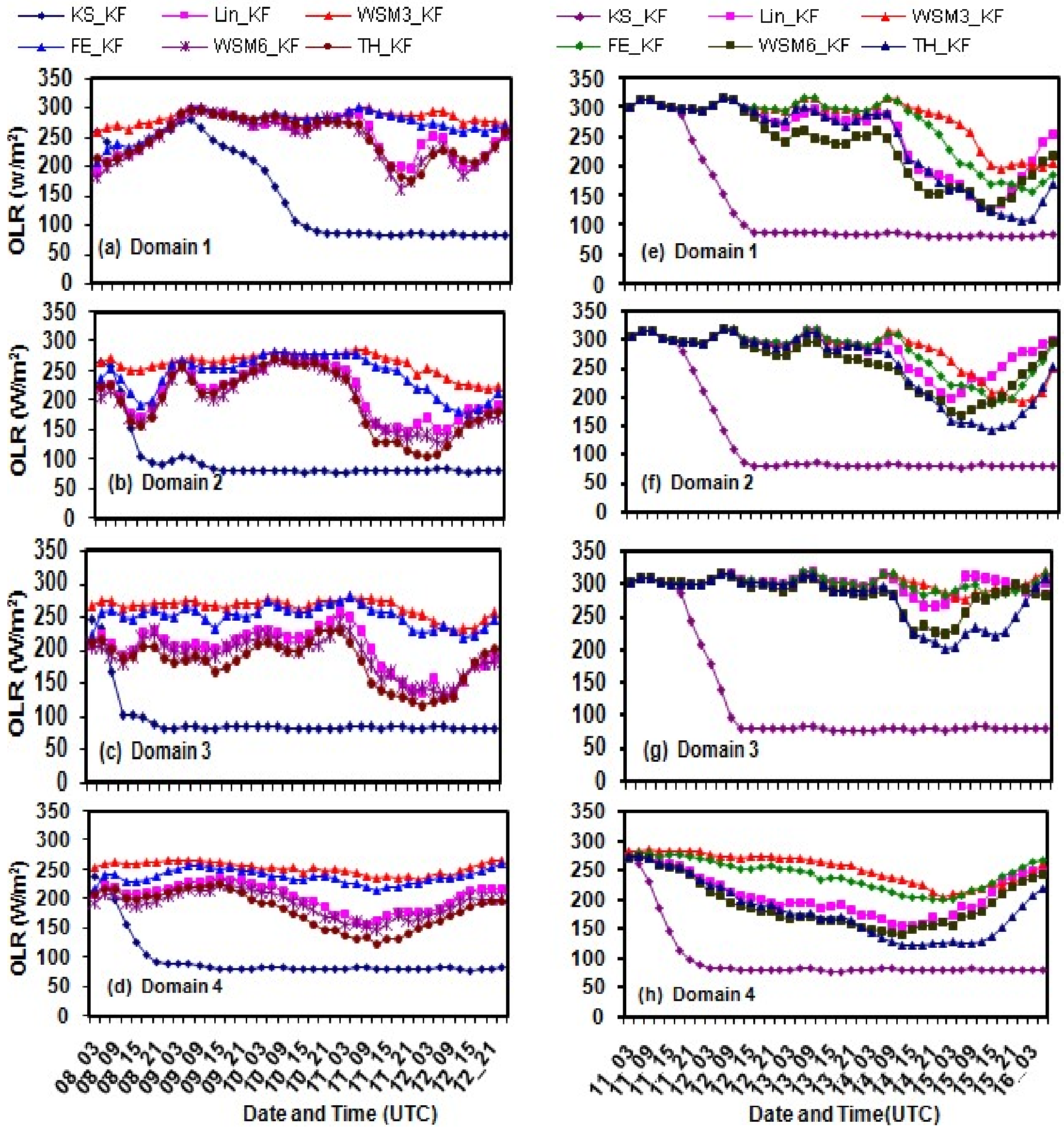

Figure 6: Model simulated OLR (W/m^2) for six different MP schemes at regions D1, D2, D3 and D4 coupling with KF scheme of (a-d) TC Phailin and (e-h) TC Sidr respectively.

The simulated OLR has exhibited an oscillatory pattern from initial to 0600 UTC at 10 October in region D2 of TC Phailin except FE and WSM3 schemes (Figure 6b). Maximum area averaged value simulated is 270 Wm^{-2} during 0600 UTC to 2100 UTC of 10 October. After that the area averaged OLR decreases sharply and reaches at minimum value of 107 Wm^{-2} at 0300 UTC on 12 October. The vertically space averaged of OLR is found to have oscillatory pattern from initial to 0300 UTC of 11 October in Figure 6c. After that the area averaged has started to decrease gradually and reached a minimum value of 116.663 Wm^{-2} at 0300UTC of 12 October.

The vertically integrated area averaged OLR has exhibited almost similar pattern of all MPs in combination with KF scheme from 0000 UTC of 8 to 1200 UTC on 12 November in regions D1, D2 and D3 as presented in Figures 6(e-g). In these Figures, the simulated output pattern is found be sinusoidal from 1200 UTC of 12 to 0600 UTC on 14

November after that it has decreased sharply in regions D1, D2 and D3 for TC Sidr. The OLR has decreased since 0600 UTC on 14 October up to crossing time of TC Sidr and reached minimum value of 106.906 Wm^{-2} in region D1 (Figure 6e) and after that it has increased. The OLR has started to decrease from 0600 UTC of 14 November but the minimum value has found to be 141.28 Wm^{-2} and 201.176 Wm^{-2} in regions D2 and D3 as shown in Figure 6(f-g). In the Oceanic region, space averaged OLR has found similar pattern for TC Phailin and Sidr except 0000 UTC of 8 to 1800 UTC on 9 October of TC Phailin.

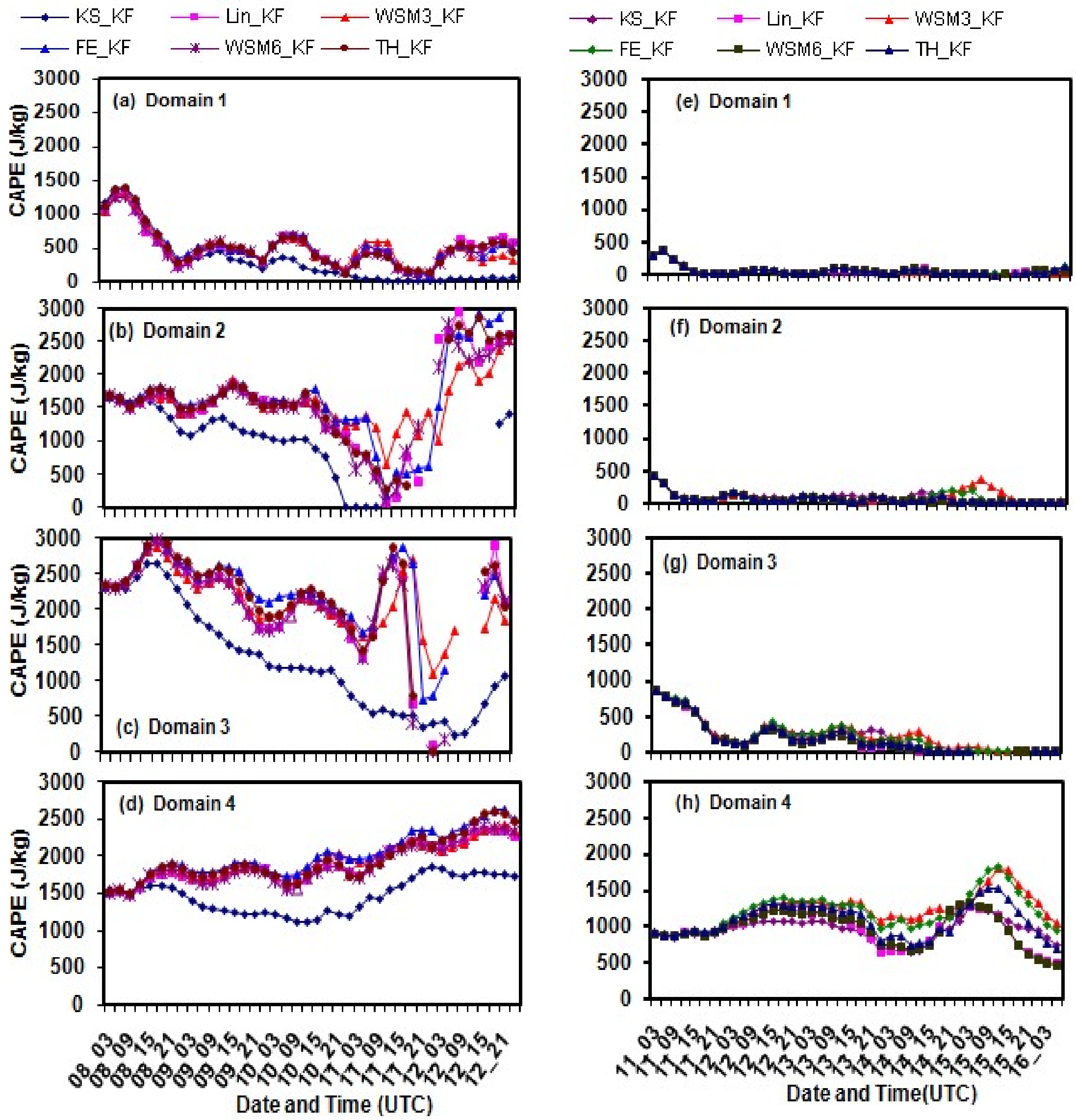

Figure 7: Model simulated area average convective available potential energy (J/Kg) for six different MP schemes in regions D1, D2, D3 and D4 coupling with KF scheme of (a-d) TC Phailin and (e-h) TC Sidr respectively.

3.4 Convective Available Potential Energy

Figure 7(a-h) shows vertically integrated space averaged convective available potential energy (CAPE) in regions D1, D2, D3 and D4 for six different MP schemes coupling with KF scheme for TCs Phailin and Sidr. Firstly, CAPE has simulated an area average maximum value of 1396.36 Jkg^{-1} at 0900 UTC of 8 October in region D1 in Figure 7a. After that the area average showed an oscillatory pattern with a crest found at 1200 UTC and trough found at 0000 UTC during the simulated time. Sinusoidal pattern has shown from initial 0000 UTC of 8 to 1200 UTC of 10 October for Phailin in region D2. In Figure 7b shows area average minimum value of 109.608 Jkg^{-1} at 1200 UTC on

11 October. The simulated area average of CAPE has maximum with 2942.2 Jkg^{-1} during the time of landfall in the region D2. For the region D3, the area average CAPE has maximum with 3032.68 Jkg^{-1} during 1800 UTC of 8 October as can be seen from Figure 7c. After that the area averaged CAPE shows a downward oscillatory pattern from 1800 UTC of 8 to 0600 UTC of 11 October. The value of area average CAPE in region D3 has increased sharply from 0600 UTC of 11 October to 1500 UTC of 11 October and decreased at around 1800 UTC at same days for Phailin. The space averaged CAPE is also found minimum with a value of 27.5931 Jkg^{-1} at 0300 UTC on 12 October in region D3. In the Oceanic region D4 shown in Figure 7d, the area average CAPE is found to have an increasing tendency wave like pattern which crest pointed at 1800-2100 UTC and trough is found at 0300-0600 UTC.

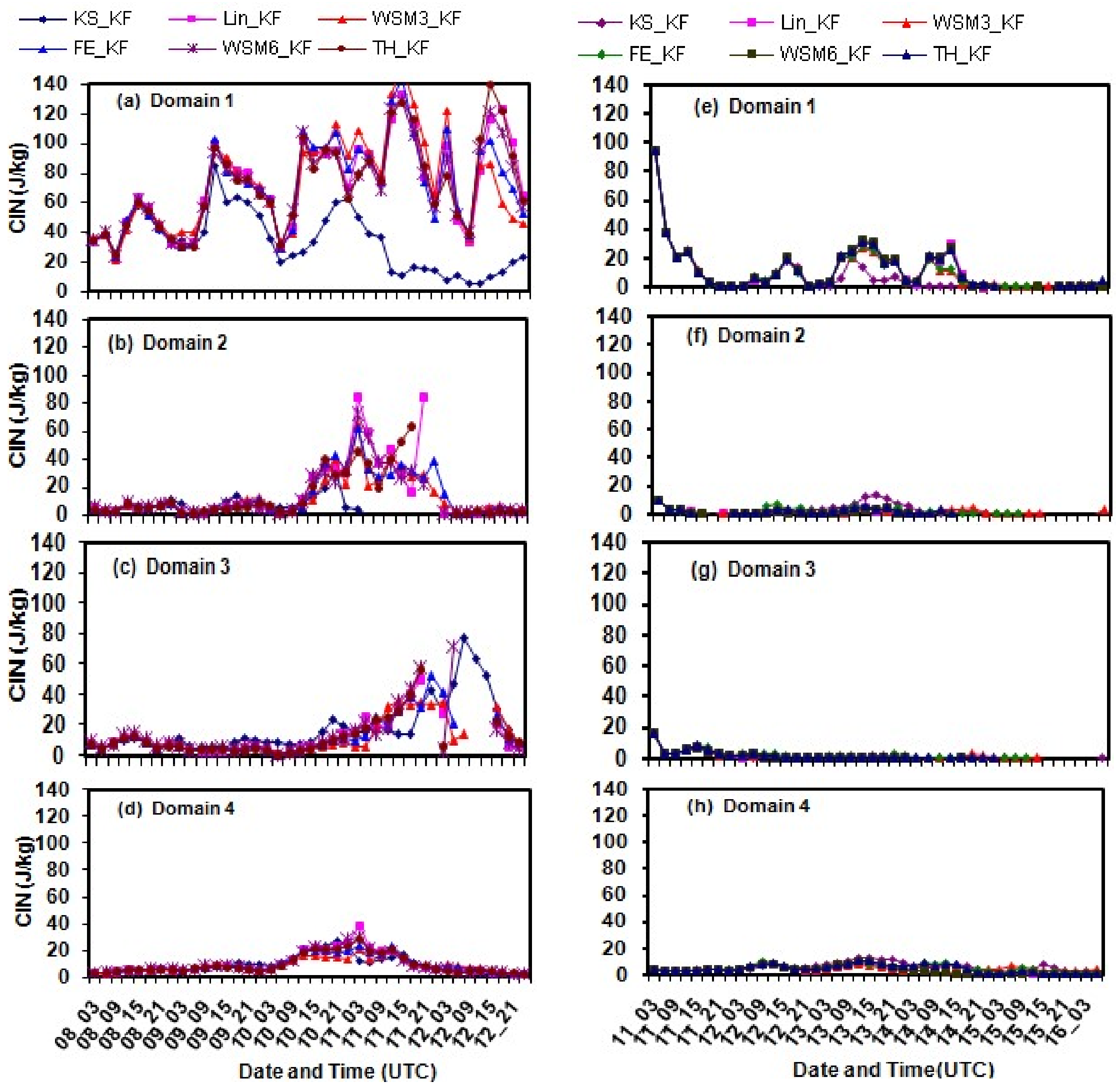

Figure 8: Model simulated area average convective inhibition (J/Kg) for six different MP schemes at domains D1, D2, D3 and D4 coupling with KF scheme for (a-d) TC Phailin and (e-h) TC Sidr respectively.

There is no significant change in area average CAPE in regions D1 and D2 as shown in the Figure 7(e-f) for Sidr. The simulated area averaged CAPE is found maximum initially with 866.665 Jkg^{-1} in the region D3 as shown in Figure 7g. After that the CAPE is found to decrease gradually up to 0600 UTC of 12 November. It's variation is an oscillatory pattern from 0600 UTC of 12 November to 1800 UTC of 14 November and then it becomes zero in region D3 as can be seen in Figure 7g. In the Oceanic region, the CAPE is found maximum with magnitude of 1823.28 Jkg^{-1} in the region D4 at the crossing time of TC Sidr. In this region D4, the simulated area average CAPE shows a constant result at fast and then it has increased from 1800 UTC on 11 November. Figure 7h also shows a minimum CAPE of 634.359 Jkg^{-1} at 0000 UTC of 14 November for Lin e*t al*. scheme in combination with KF scheme. Yin *et al.* (2014) have found that dry air produces lower CAPE. CAPE is effectively the positive buoyancy of an air parcel and is an indicator of atmospheric instability, which makes it very valuable in predicting severe weather. So, low value of CAPE in regions D1, D2, D3 indicates lower speed and moist in case of Sidr as compared with Phailin. But in region D4, both cyclones have high area average CAPE values that vary differently with respect to each other.

3.5 Convective Inhibition

The simulated area averaged convective inhibition (CIN) for TCs Phailin and Sidr for six different MP schemes coupling with KF scheme in region D1, D2, D3 and D4 are presented in Figure 8(a-h). The time varying area averaged of CIN shows a zigzag pattern for Phailin in region D1. In the region, a maximum value of 140 Jkg^{-1} of CIN is observed at 1500 UTC on 12 October and a minimum value of 24 Jkg^{-1} at 0900 UTC of 08 October. Because of its zigzag pattern it has no regular crest and trough. The simulated space averaged CIN has about the same pattern from 0000 UTC of 8 October to 1200 UTC of 10 October for the regions D2 and D3 as can be seen in Figure 8b and 8c. After that CIN has increased sharply and reached at maximum value for all MP's in combination with KF scheme in region D2. In the region D3, CIN has increased gradually and become discrete at end time of Phailin. The simulated area averaged CIN is found to have an insignificant value except at 0300 UTC of 10 October to 0000 UTC of 12 October in the region D4 (Figure 8d). The peak value of CIN is 38.55 Jkg^{-1} observed at this Oceanic region D4.

For the TC Sidr in region D1, CIN has decreased from 0000 UTC of 11 to 1800 UTC of 11 November (Figure 8e). It has shown an oscillatory pattern from 0900 UTC of 12 November to 1800 UTC of 14 November in the region D1 of TC Sidr. After that CIN has become zero up to landfall Figure 8e. There is no significant value of CIN for TC Sidr in the regions D2, D3 and D4 during the simulated time as compared with that in case of Phailin (Figure 8(f-h)). CAPE and CIN have shown an inverse relation with moist and dry air (Gettelman e*t al.,* 2002; Myoung and Nielsen-Gammon, 2010; Santanello e*t al.,* 2011). The area average CIN of both TCs has no significant variation for the prediction of track.

4. CONCLUSIONS

- The simulated central SLP for all MP schemes coupling with BMJ scheme with the initial conditions at 0000 UTC of 9 October 2013 matched with IMD observed pressure fall but much higher than that of JTWC observed results.
- The JTWC observed 10 m level wind speed (33 m/s) with the initial conditions at 0000 UTC 9 October is found to match with Kessler-KF (32.9 m/s) combination.
- The simulated tracks of TC Phailin for all MP schemes in combination with KF scheme indicates almost no track error at the time of landfall with the initial conditions at 0000 UTC of 9 October. There is almost no time lag by Kessler, Lin, WSM3, WSM6 and Thompson schemes in combination with KF scheme with the initial conditions of 0000 UTC on 8 October.
- The landfall time of TC Sidr has almost matched for all MP schemes in combination with BMJ scheme, and Lin *et al*. and WSM6 schemes in combination with KF scheme for the initial conditions of 0000 UTC 11 November. There is no landfall of TC Sidr up to the simulation time for WSM3 scheme in combination with KF and BMJ schemes with the initial conditions of 0000 UTC of 11 and 12 November 2007.
- The OLR has fallen in all four regions for both TCs one day before crossing the land and becomes minimum in case of Sidr and Phailin in regions D1 and D2 compared to other regions.
- The simulated area averaged CAPE is found to have sharp decreasing pattern in regions D2 and D3 for TC Phailin and in D3, D4 for TC Sidr before landfall.
- Minimum CIN is found before crossing the land in regions D2, D3 and D4 but maximum at D1 for Phailin. For TC Sidr, insignificant CIN is found in four regions as compared with that in case of Phailin. CIN is maximum one day before for TC Phailin in regions D2 and D3. CIN has maximum values all the time in region D1 for TC Phailin. In Oceanic region D4, CIN has found similar pattern for TC Phailin and Sidr.
- On the basis of above findings for the convective parameters CAPE and CIN, it is difficult to say in which region the tropical cyclone will likely to move. But the OLR has shown a significant result for the movement of tropical cyclone. Further research will require for identifying the effects of these parameters for movement of tropical cyclones.

ACKNOWLEDGEMENT

The authors acknowledge the Mesoscale and Microscale Meteorology Division of National Center for Atmospheric Research (NCAR) for providing WRF-ARW model. The Grid Analysis and Display System (GrADS) and Microsoft Excel was used for analytical purpose. The authors are grateful to Indian Meteorological Department (IMD) and Joint Typhoon Warning Center (JTWC) for using their data in this study.

REFERENCES

Bogner, P. B., Barnes, G. M. and Franklin, J. L., 1999. Conditional instability and shear for six Hurricanes over the Atlantic Ocean, *Amer. Meteor. Soc.,* 15, 192-207.

Camargo, S. J., Robertson, A. W., Gaffney, S. J., Smyth, P. and Ghil, M., 2007. Cluster analysis of Typhoon tracks. Part II: Large-Scale Circulation and ENSO, *J. Climate,* 20, 3654-3676.

Choi, K. S. and Moon, I. J., 2012. Changes in tropical cyclone activity that has affected Korea since (1999)*, Nat. Hazards*, 62, 971–989.

Choi, K. S., Byun, H. R., 2010. Possible relationship between western North Pacific tropical cyclone activity and Arctic Oscillation, *Theor Appl Climatol* 100, 261–274.

Colon-pagan, I. C., 2009. Orographic effects on rainfall induced by the passage of Tropical Cyclones over Mountainous Islands: Part I: The Effect of Cloud Microphysics, *SOARS,* 1-25.

Evans, J. L., and Waters, J. J., 2012. Simulated relationships between sea surface temperatures and Tropical convection in climate models and their implications for tropical cyclone activity, *J. Climate,* 25, 7884–7895.

Fang, J., Tang, J. P. and Wu, R. S., 2009. The effect of surface friction on the development of tropical cyclones, *Adv. Atmos. Sci.,* 26(6), 1146–1156.

Gettelman, A., Seidel, D. J., Wheeler, M. C., and Ross, R. J., 2002. Multidecadal trends in tropical convective available potential energy, *J. Geophys. Res*., 107(D21), 4606, doi:10.1029/2001JD001082.

Molinari, J. and Vollaro, D., 2009. Notes and correspondence distribution of helicity, CAPE, and shear in Tropical Cyclones, *J. Atmos. Sci.,* 67, 274-284.

Myoung, B. and Nielsen-Gammon, J. W., 2010. The convective instability pathway to warm season drought in Texas. Part I: The role of convective inhibition and its modulation by soil moisture*, J. Clim.,* 23, 4461-4473.

Nolan, D. S., Rappina, E. D. and Emanuel, K. A., 2007. Tropical cyclogenesis sensitivity to environmental parameters in radiative–convective equilibrium, *Q. J. R. Meteorol. Soc.,* 133, 2085–2107.

Pattanaik, D. R. and Rama Rao, Y. V., 2009. Track prediction of very severe cyclone 'Nargis' using high resolution weather research forecasting (WRF) model, *J. Earth Syst. Sci.,* 118(4), 309–329.

Santanello, J. A., Peters-Lidard, C. D. and Kumar, S. V., 2011, Diagnosing the sensitivity of local land-atmosphere coupling via the soil moisture-boundary layer interaction*, J. Hydrometeorol,* 12, 766-786. doi:10.1175/JHM-D-10-05014.1

Smith, R. K. and Montgomery, M. T., 2012. A Observations of the convective environment in developing and non-developing tropical disturbances, *Q. J. R. Meteorol. Soc.,* 138, 1721-1739.

Sobel, A. H. and Camargo, S. J., 2005, Influence of Western North Pacific Tropical Cyclones on Their Large-Scale Environment, *J. Atmos. Sci.,* 62, 3396-3407.

Xu, J. and Wang, Y., 2010. Sensitivity of Tropical Cyclone Inner-Core Size and Intensity to the Radial Distribution of Surface Entropy Flux Journal of the Atmospheric Sciences, *J. Atmos. Sci.,* 67(6), 1831-1852.